

# Gamma-Ray Bursts and Magnetars as Possible Sources of Ultra High Energy Cosmic Rays: Correlation of Cosmic Ray Event Positions with IRAS Galaxies

Shwetabh Singh,<sup>\*</sup> Chung-Pei Ma,<sup>†</sup> and Jonathan Arons<sup>‡§</sup>

*Department of Astronomy and Theoretical Astrophysics Center,  
University of California, Berkeley,  
601 Campbell Hall, Berkeley, CA 94720*

We use the two-dimensional Kolmogorov-Smirnov (KS) test to study the correlation between the 60 cosmic ray events above  $4 \times 10^{19}$  eV from the AGASA experiment and the positions of infrared luminous galaxies from the IRAS PSCz catalog. These galaxies are expected to be hosts to gamma ray bursts (GRB) and magnetars, both of which are associated with core collapse supernovae and have been proposed as possible acceleration sites for ultra high energy cosmic rays. We find consistency between the models and the AGASA events to have been drawn from the same underlying distribution of positions on the sky with KS probabilities  $\gtrsim 50\%$ . Application of the same test to the 11 highest AGASA events above  $10^{20}$  eV, however, yields a KS probability of  $< 0.5\%$ , rejecting the models at 99.5% significance level. Taken at face value, these highest energy results suggest that the existing cosmic ray events above  $10^{20}$  eV do not owe their origin to long burst GRBs, rapidly rotating magnetars, or any other events associated with core collapse supernovae. The larger data set expected from the AUGER experiment will test whether this conclusion is real or is a statistical fluke that we estimate to be at the  $2\sigma$  level.

## I. INTRODUCTION

The source of cosmic rays at energies above the Greisen-Zatsepin-Kuzmin (GZK) feature [1], predicted to appear at energies above  $\sim 4 \times 10^{19}$  eV, remains a mystery [2]. These events have been seen by the Akeno Giant Air Shower Array (AGASA) [3], Fly's Eye [4], Haverah Park [5], HiRes [6], and Yakutsk [7] experiments. Interaction of charged as well as neutral primaries with the cosmic background photons through photo-production of pions, photo-pair production, and inverse Compton scattering [8] leads to a severe energy degradation and constrains the source of a  $\sim 10^{20}$  eV charged particle to distances less than  $\sim 50$  Mpc (the high energy GZK zone). The lack of the most commonly hypothesized accelerators *viz.* accretion disks and jets associated with active galactic nuclei within the GZK zone has led to numerous alternate proposals for the origin of the Ultra-High Energy Cosmic Rays (UHECRs).

These explanations fall into two broad categories of top-down and bottom-up scenarios. Top-down models generally rely on the decays of very heavy particles, usually remnants from the early universe [2]. Bottom-up models are based on the acceleration of normal charged particles to extremely high energies in astrophysical objects not otherwise known to possess such effective acceleration mechanisms [9]. These accelerators are expected to show a correlation with some known class of astrophysical objects in the local universe.

Supernovae and their remnants have long been suspected as the source of ordinary cosmic rays below  $4 \times 10^{19}$  eV. Two models based on gamma ray bursts (GRBs) and magnetars for the acceleration of UHECRs have been proposed that attribute these particles to brief bursts of particle emission associated with the formation of compact objects in core collapse supernovae. In the GRB model, Milgrom and Usov [10], Vietri [11] and Waxman [12] independently suggested that the relativistic shock waves associated with GRBs might be the acceleration sites for these cosmic rays. The relativistic shock model has been useful in accounting for the phenomenology of GRBs [13]. Recent observations of GRB afterglows have supplied strong evidence that at least the long burst sources are associated with supernovae occurring in external galaxies [14]. The prompt association of the afterglow of GRB030329 with SN2003dh gives strong support to the prompt formation of the collapsed object that drives the outburst, either a black hole, as in the collapsar model [15], or a rapidly rotating magnetar [16]; the latter model works only if the jet that drives the GRB contains only part of the rotational energy delivered, with the rest driving the supernova envelope, as in the magnetar model for UHECRs proposed in Ref. [17].

Arons [17] showed that magnetars, a sub-class of neutron stars with ultra strong surface magnetic fields ( $B \sim 10^{15}$  Gauss) born in core collapse supernovae and hypothesized to have initial spin rates close to the centrifugal breakup limit, are unipolar inductors that can accelerate particles in their relativistic winds up to energies  $\sim 10^{22}$  eV. They have an electrodynamically defined injection rate sufficient to yield a quantitatively acceptable account of the observed UHE spectrum, if such events occur in external galaxies with core collapse supernovae. Blasi, Epstein, and Olinto [18] presented a galactic pulsar variant of this idea, and Milgrom and Usov [10] earlier

<sup>‡</sup>also Physics Department, University of California, Berkeley

<sup>\*</sup>shwetabh@astro.berkeley.edu

<sup>†</sup>cpma@astro.berkeley.edu

<sup>§</sup>arons@astro.berkeley.edu

showed that such objects have voltages (including voltage drops in the wind) large enough to account for the maximum energies seen in UHECR. Since some of the magnetars in our galaxy are physically associated with supernova remnants [19], the association of magnetars with core collapse supernovae is plausible.

Since both the GRB and magnetar models attribute UHECRs to compact objects formed in core collapse supernovae (probably in the Ib/c sub-class), the rate of events that give rise to UHECRs in a galaxy should be proportional to the supernova rate in galaxies that have core collapse supernovae. Likewise, the core collapse supernova rate has been observed to be strongly correlated to the star formation rate (SFR) [20], a correlation readily understood from the fact that such supernovae have short lived, massive stellar progenitors. This correlation leads us to explore the connection between the UHECR events and infrared bright spirals that are known to be active star forming regions.

In this paper we test the hypothesis that the origin of the UHECR events lies in reasonably prompt acceleration following a core collapse supernova, by studying the correlations between the angular locations of UHECR events on the sky and the positions of galaxies with a high SFR using the two-dimensional Kolmogorov-Smirnov (KS) test. We choose the IRAS Point Source Catalogue (PSCz) for our galaxy sample [21]. The catalogue consists of 14800 galaxies with measured redshifts and far infrared luminosities above a flux limit of 0.6 Jansky at  $60\mu m$ . The sky coverage is  $\sim 84\%$ .

Sec II provides a summary of the acceleration theories. Sec III discusses observational and theoretical evidence for the expected formation rate of the relevant compact objects in infrared bright spirals, and discusses the use of the IRAS PSCz catalogue and the AGASA sample in our study. Sec IV describes the statistical methods and results on the data and theoretical models. Sec V and VI provide further discussion and conclusion of our results.

## II. COMPACT OBJECT PARTICLE ACCELERATION THEORY

### A. Gamma Ray Bursts

Gamma ray bursts, and especially their afterglow emission, clearly reflect the excitation of the magnetized gaseous medium surrounding an explosive release of energy from a compact object of at least stellar mass [13]. The observed relativistic expansion rates (*e.g.*, [22]) support that release having given rise to relativistic outflow, well modeled in the afterglow phase as a relativistic blast wave propagating through a surrounding circumstellar or interstellar medium. In analogy to the apparent ability of ordinary supernova remnant shocks to accelerate a small fraction of the particles in the surrounding medium to relativistic energies, the authors in Refs. [10], [11], [12] suppose that relativistic shocks, either that of an external

blast wave expanding with Lorentz factor  $\gamma \sim 100 - 1000$  which creates the afterglow or those of the internal shocks with  $\gamma \sim 2 - 10$  associated with the prompt GRB, are responsible for the acceleration of the UHECR. The luminosity density for UHECR is  $\dot{U}_{\text{UHE}} \sim 5 \times 10^{44}$  ergs/Mpc<sup>3</sup>-sec [17, 23], about a factor of 5 greater than the photon luminosity density of GRBs ( $\sim 10^{44}$  ergs/Mpc<sup>3</sup>-sec [23] but well below the mechanical luminosity density of GRBs,  $\sim 10^{46}$  ergs/Mpc<sup>3</sup>-sec, assuming  $\sim 1\%$  efficiency in converting internal shock energy into photon energy [24]. The synchrotron model of GRB emission provides the only evidence for particle energies in a GRB or its afterglow large enough to correspond to ions being at relativistic energies.

The energetics of this model are demanding but not exorbitant. The total observed GRB rate is  $n_g^{\text{GRB}} \nu_{\text{GRB}} f_b \sim 0.5 \times 10^{-9}$  Mpc<sup>-3</sup> yr<sup>-1</sup> [25], where  $n_g^{\text{GRB}}$  is the number density of galaxies hosting GRBs,  $\nu_{\text{GRB}}$  is the GRB rate per host galaxy, and  $f_b = \Omega_b/4\pi$  is the fraction of the outflow beamed into solid angle  $\Omega_b$ , with  $f_b \sim 0.01$  inferred in many afterglows. Long bursts provide about 70% of the observed GRB rate [26], that is,  $n_g^{\text{SNe}} \nu_{\text{GRB}} \sim 0.35 \times 10^{-9}$  Mpc<sup>-3</sup> yr<sup>-1</sup>/ $f_b$ , where  $n_g^{\text{SNe}}$  is the number density of galaxies with core collapse supernovae  $n_g^{\text{SNe}}$ , and  $\nu_{\text{GRB}}$  is some fraction of the overall core collapse supernova rate per galaxy. Then the UHE energy demanded of each burst source, if long bursts are the sole contributors, is  $\Delta E_{\text{UHE}}^{\text{GRB}} = \dot{U}_{\text{UHE}}/n_g^{\text{SNe}} \nu_{\text{GRB}} = 10^{54} f_b$  ergs =  $10^{52} (f_b/0.01)$  ergs. This energy is somewhat in excess of the energy put into photons in each burst. As is obvious from the energy budget of rotation powered pulsars and, to a lesser extent, of AGN with well developed jets, there is no fundamental difficulty with particle acceleration power exceeding photon luminosity in a compact object, especially if the outburst draws its power from the pressure of large scale electromagnetic fields.

The microphysics arguments advanced for GRBs being a source of UHECR depends on the theory of particle acceleration in shocks. Most authors have employed the much studied theory of diffusive Fermi acceleration in shocks in the test particle limit to estimate maximum energies and spectra, with the efficiency of shock acceleration left as a free parameter. Here, we reiterate the well known remark [27] that the maximum energy a charged particle can attain in a relativistic shock wave is  $\sim ZeBR_s = 3 \times 10^{20} B_{10} R_{s17}$  eV, where  $Z$  is the atomic number of the charged particle,  $e$  is the electronic charge,  $B_{10}$  is the *systematic* magnetic field of the medium into which the shock propagates in units of 10 Gauss, and  $R_{s17}$  is the radius of the shock wave in units of  $10^{17}$  cm;  $R_{s17} \sim 1$  is typical of the shock size during afterglow emission. This energy corresponds to a particle's Larmor radius having reached the size of the shock, at which point the particle can move through the motional electric field as a freely accelerating particle and experience the full electric potential drop. Acceleration at internal shocks, which occur at much smaller radii, re-

quire concomitantly larger magnetic fields, if GRBs are to be the acceleration sites for the highest energy particles. Such fields are *much* larger than found anywhere in the interstellar media of galaxies, forcing the proponents of this model to appeal to relativistic shock propagation in unusual environments, such as the  $B \propto r^{-1}$  field in the possibly strongly magnetized circumstellar winds which might surround a presupernova star [28] or the similarly structured field in the relativistic wind from a newly formed neutron star (Ref. [23] and references therein) or from a transient magnetized disk around a newly formed black hole (Ref. [15]).

Granted the existence of such environments, the particle spectrum created by such a shock may be a power law with  $f(E) = E^{-p}$ ,  $p = 2 - 2.5$ ; detailed studies of the test particle problem yield  $p = 2.2 - 2.3$  [29]. Models of the acceleration physics which incorporate some information about the magnetic turbulence that scatters downstream particles back across the shock front indicate possibly steeper spectra [30]. Such turbulence is an essential ingredient if the mechanism as applied to shocks with flow Lorentz factors less than  $10^3$  are to accelerate particles to UHECR energies. The efficiency with which such shocks can convert flow energy into accelerated particle spectra is unknown, although judging from the acceleration efficiencies for electrons and positrons found in the much more highly relativistic shocks terminating the winds from rotation powered pulsars, efficiencies as high as 1-10% appear possible [31].

## B. Magnetars

Magnetars are a special class of neutron stars which form in core collapse supernovae. Studies of their association with supernova remnants in our own galaxy suggest the overall birth rate of magnetars is on the order of 1-10% of the total core collapse supernova rate [19]; this rate is comparable to the rate of type Ib/c supernovae. Therefore, the magnetar birth rate is in effect proportional to the supernova rate in a galaxy. The theory described in [17] suggests injection of charged particles with maximum energy

$$E_{\max} = Ze\Phi_i = Ze \frac{B_* \Omega_i^2}{R_*^3 c^2} = 3 \times 10^{22} Z B_{15} \Omega_4^2 \text{ eV}. \quad (1)$$

Here  $B_*$  is a magnetar's surface magnetic field,  $B_{15} = B_*/10^{15}$  Gauss,  $\Omega_i = 10^4 \Omega_4 \text{ s}^{-1}$  is the initial angular velocity of the neutron star,  $R_*$  is the stellar radius, and  $c$  is the speed of light. The initial rotation period is  $P_i = 0.64/\Omega_4$  msec. The ions actually gain their energy in the relativistic wind electromagnetically expelled from the neutron star at distances,  $r$ , much larger than the radii of the star and its magnetosphere, which allows them to avoid catastrophic radiation losses; the electric potential in the wind is  $rE = rB = \Phi$ . If  $Z = 1 - 2$ , as may be suggested by the shower data [2], one requires  $P_i < 2 - 3$

msec for the model to be viable. Studies of the termination shocks of pulsar winds show that the relativistic ions gain their energy in the wind interior to the winds' termination shocks, rather than at that (reverse) shock, or at the blast wave driven into the surrounding interstellar medium [32]. The magnetar model in [17] adopts this acceleration site by analogy to pulsars, rather than appealing to the relativistic blast wave driven by a newly born magnetar's fields into the surrounding interstellar medium.

The star spins down rapidly, under the influence of electromagnetic and gravitational wave torques. As it spins down, the voltage and the particle energies decline. Summing over the formation and spindown event, one finds a per event injection spectrum proportional to  $f(E) = E^{-1}[1 + (E/E_g)]^{-1}$  for  $E < E_{\max}$ . Here  $E_g$  measures the importance of gravitational wave losses (calculated for a star with static non-axisymmetric quadrupole asymmetry) in spinning the star down. These losses have significance only at the largest rotation rates, if they matter at all. When they exert torques larger than the electromagnetic torque, the star spends less time at the fastest rotation rates and therefore spends less time accelerating the highest energy particles, thus causing a steepening in the spectral slope at the highest energies. If the star has an internal magnetic field even stronger than the already large surface field, equatorial ellipticities  $\epsilon_e$  in excess of  $10^{-3}$  can exist, in which case  $E_g$  would be less than  $E_{\max}$ . We consider three cases of energy loss due to gravitational radiation (GR) in the model: no GR loss ( $\epsilon_e = 0, E_g = \infty$ ); moderate GR loss ( $\epsilon_e = 0.01, E_g = 3 \times 10^{20} \text{ eV}$ ); strong GR loss ( $\epsilon_e = 0.1, E_g = 3 \times 10^{18} \text{ eV}$ ).

The total number of particles injected per event is

$$N_i \approx 2 \frac{c^2 R_*^3 I}{Ze B_*} \approx \frac{10^{43}}{Z B_{15}}, \quad (2)$$

where we have assumed a stellar radius of 10 km and a moment of inertia  $I = 10^{45}$  cgs. In this respect, the magnetar model is much more specific than the GRB model, since the ion flux is uniquely fixed by the electrodynamics of the unipolar inductor. In order to tap the motional EMF of the wind, the particles must cross magnetic field lines and move parallel to the electric field. In Ref. [17], it was suggested that the current sheets in the structured wind are unstable to the formation of large amplitude electromagnetic waves, whose ponderomotive force drives the particles across  $B_{\text{wind}}$ , thus causing the energy gain, a mechanism analogous to those studied in the design of advanced accelerators and of some interest for ion acceleration in the observationally much better constrained pulsar winds.

The rate at which galaxies inject UHECR into the universe in this model then is  $\dot{n}_{\text{cr}} = \nu_{\text{mag}}^{\text{fast}} N_i n_{\text{galaxy}}$ , where  $n_{\text{galaxy}} \approx 0.02 \text{ Mpc}^{-3}$  [33],  $N_i$  is given by Eq. (2), and  $\nu_{\text{mag}}^{\text{fast}}$  is the birth rate of *rapidly rotating* magnetars per galaxy. If intergalactic propagation is unaffected by scattering in an intergalactic magnetic field, multiplication

of the source spectrum  $q(E) \propto \dot{n}_{\text{cr}} f(E)$  by the energy dependent GZK loss time yields a spectrum received at the Earth in reasonable accord with the existing observations of UHECR, as shown in Figure 1 of Ref. [17], if  $\nu_{\text{mag}}^{\text{fast}} \approx 10^{-5} \text{ yr}^{-1}$ . That fast magnetar birth rate lies between 1% and 10% of the total magnetar birth rate inferred for our galaxy, and about 0.1% of the total core collapse supernova rate in average star forming galaxy,  $\sim 10^{-2} \text{ yr}^{-1}$  [34].

In [17], the fast magnetar event rate was applied to all normal galaxies, whose space density is  $n_g = 0.02 \text{ Mpc}^{-3}$  [33], yielding an event rate  $n_g \nu_{\text{m}}^{\text{fast}} \sim 2 \times 10^{-7} \text{ Mpc}^{-3} \text{ yr}^{-1}$ . The luminosity density of injected energy from the wind, which is about equal to the energy expended in accelerating the ions, is  $10^{46}$ ,  $0.9 \times 10^{45}$ , and  $0.9 \times 10^{43} \text{ ergs/Mpc}^3 \text{ yr}^{-1}$ , in the no GR, moderate GR and strong GR cases, assuming the same  $\nu_{\text{m}}^{\text{fast}}$  in all three applications of the model. In fact, since  $\nu_{\text{m}}^{\text{fast}}$  is an otherwise unknown fraction of the poorly known  $\nu_{\text{m}}$ , the value of  $\nu_{\text{m}}^{\text{fast}}$  was adjusted in each case so as to provide the best agreement between the model's UHECR spectrum and the observations. The UHECR energy per event is much smaller than is required for the GRB model, whose effective rate of occurrence (including beaming) is much less than for magnetars. However, there are many normal galaxies within every resolution element of the arrays used to accumulate the UHECR events, making angular correlations between all normal galaxies and UHECR events difficult in testing the magnetar (and the long burst GRB) hypothesis for the UHECR's origin. The luminous infrared galaxies offer a better prospect for testing these models, since they are rarer than ordinary galaxies but still contribute a substantial fraction of the metagalactic supernova rate (see below).

### III. STUDY SAMPLE AND SKY COVERAGE

In this section we discuss how the far infrared luminosity of a galaxy serves as an indicator of its core collapse supernova rate and why the IRAS catalogue is chosen as the galaxy sample. We then discuss the use of AGASA events as the UHECR sample.

#### A. Infrared Galaxies

Type Ib/c and type II supernovae are considered good indicators of the SFR in a galaxy. The progenitors of these core collapse supernovae are young, massive stars that are abundant in active star forming regions. Observational support for relating the SFR to the far infrared luminosity ( $\lambda > 20 \mu\text{m}$ ) has come from study of the IRAS catalogue of  $\sim 15000$  infrared bright galaxies. The method relies on the fact that a large percentage of the bolometric luminosity of young stars is absorbed by interstellar dust and then emitted as thermal radiation from the warmed dust in the far infrared spectrum [20].

The absorption cross section of dust is strongly peaked in the ultraviolet, where the young stars dominate the radiation. This makes the thermal far infrared luminosity of a galaxy a good proxy for the SFR.

Specifically, we take the supernova rate and therefore the birth rate of stellar mass collapsed objects to be proportional to the luminosity of a galaxy at  $60 \mu\text{m}$ . This wavelength is chosen to reduce the contamination from the radiation field of older stars at  $\lesssim 10 \mu\text{m}$  as well as the cirrus emission at  $\gtrsim 100 \mu\text{m}$  due to stellar optical/near IR radiative excitation of large molecules in the interstellar medium [20].

Luminous infrared galaxies with high SFRs and supernova rates offer the best chance of finding a correlation between UHECR event source directions and sites of core collapse supernovae. We use the IRAS PSCz catalogue [21] as the host galaxies for GRBs and magnetars. This catalogue has a nearly uniform coverage of  $\sim 84\%$  of the sky, where most of the unmapped area lies within  $\sim 10^\circ$  north and south of the galactic plane. The sample provides redshifts for all galaxies above a flux limit of 0.6 Jansky at  $60 \mu\text{m}$ .

These galaxies contribute a substantial fraction of the overall core collapse supernova rate. From the IRAS catalogue, these objects have space density  $dn_{\text{firg}}/dL_{10} \approx 10^{-3} L_{10}^{-1 \pm 0.1} \text{ Mpc}^{-3}$ , where  $L_{10} = L_{\text{FIR}}/10^{10} L_\odot$  and  $L_{\text{FIR}}$  is the far infrared luminosity [35]. The integral number of these galaxies ( $1 < L_{10} < 10^3$ ) is  $n_{\text{firg}} \approx 0.005 \text{ Mpc}^{-3}$ , which should be compared to the total space density of galaxies,  $n_g \approx 0.02 \text{ Mpc}^{-3}$  [33]; most of these are spirals and other galaxies with some degree of ongoing star formation.

The general core collapse supernova rate per galaxy, summed over all galaxy types, is  $\dot{S}_{\text{sn}} \approx 0.011 \text{ SN per galaxy-year}$  [34], which yields a volume averaged rate of supernovae of  $\dot{S}_{\text{sn}} n_g \approx 2.2 \times 10^{-4} \text{ SN/Mpc}^3 \text{ year}$ . The supernova rate for galaxies with far infrared emission is  $\dot{S}_{\text{sn}}^{\text{fir}} = 2.5 \times 10^{-4} L_{10} \text{ SN/(FIR galaxy)-year}$  [36]. Integrating this supernova rate over the FIR galaxy luminosity function yields  $\dot{S}_{\text{sn}}^{\text{fir}} n_{\text{firg}} \approx 0.7 \times 10^{-4} K_{\text{obsc}} (L_{10}^{\text{max}}/300) \text{ SN/Mpc}^3 \text{ year}$ .  $K_{\text{obsc}}$ , the correction for supernovae missed in the existing optical and near infrared supernova detection surveys, might be as large as 10, and probably is at least as large as 3 [36]. Thus, the luminous infrared galaxies contribute at least 28% ( $K_{\text{obsc}} = 1$ ) of the total supernova rate, with a total space density only 25% that of all normal galaxies. Furthermore, since the brightest infrared galaxies ( $L_{\text{FIR}} > 10^{12} L_\odot$ ) dominate the contribution from all FIR galaxies, and these are quite rare, with space density  $\sim 4 \times 10^{-8} \text{ Mpc}^{-3}$  [35], correlations of UHECR arrival directions with the sky positions of the luminous IRAS galaxies offers a promising opportunity to test the hypothesis that UHECR acceleration has something to do with core collapse supernovae, as is implied by the GRB shock and magnetar unipolar inductor models for the acceleration sites.

## B. UHECR Events

For the UHECR events, we choose the AGASA experiment because among the ground based arrays, this experiment has the best angular resolution ( $1.8^\circ$  FWHM [37]) and provides the largest single dataset above  $4 \times 10^{19}$  eV. The current sample of AGASA UHECR events contains 60 events above  $4 \times 10^{19}$  eV, among which 57 events are published in Ref. [38] and 3 recent events with energies greater than  $1 \times 10^{20}$  eV are listed at the AGASA website [39].

In order to test whether the AGASA events are consistent with their origin being from IRAS galaxies, we must first take into account the different sky coverage by AGASA vs. IRAS and the possible variations in detector exposure efficiency in AGASA. Continuously operating ground-based arrays such as AGASA typically have a uniform coverage in sidereal time and therefore little exposure variations in right ascension (RA) [37]. The detector exposure in declination, however, depends on the latitude  $\theta_0$  of the experiment and drops to zero beyond certain maximum angle,  $\theta_{\max}$ . For AGASA,  $\theta_0 = 35.8^\circ$  and  $\theta_{\max} = 45^\circ$ . Beyond  $45^\circ$ , the energy determination of the events becomes uncertain. In terms of these parameters, the detector efficiency as a function of declination,  $\theta$ , is given by [40, 41],

$$\frac{dN_t}{d\theta} \propto (\cos \theta_0 \cos \theta \sin \alpha_m + \alpha_m \sin \theta_0 \sin \theta), \quad (3)$$

where  $\alpha_m$  is given by

$$\alpha_m = \begin{cases} 0, & \text{if } \xi > 1 \\ \pi, & \text{if } \xi < -1 \\ \cos^{-1} \xi, & \text{otherwise} \end{cases} \quad (4)$$

and

$$\xi \equiv \frac{\cos \theta_{\max} - \sin \theta_0 \sin \theta}{\cos \theta_0 \cos \theta}. \quad (5)$$

For comparison, we find the observed declination distribution published in Ref. [37] for the number of AGASA events above  $1 \times 10^{19}$  eV to be well fit (to  $\sim 1\%$ ) by

$$\frac{dN_o}{d\theta} = \begin{cases} -(\theta + 10)(\theta - 80)/35.5, & \text{if } -10^\circ < \theta < 80^\circ \\ 0, & \text{otherwise} \end{cases} \quad (6)$$

We have verified that the declination distribution for events above  $4 \times 10^{19}$  eV is similar to Eq. (6). This is consistent with the triggering efficiency being uniform above  $1 \times 10^{19}$  eV and the UHECR events not showing any appreciable large scale anisotropy [37, 42, 43]. We use the theoretical window function in Eq. (3) for the statistical tests in Sec. IV and discuss the implications of using the observed declination distribution in Sec. V.

Fig. 1 shows the sky distribution of the AGASA UHECR events and the area not mapped in the PSCz

catalogue. Six AGASA events lie in these unmapped regions and will therefore be excluded, leaving 54 AGASA data points above  $4 \times 10^{19}$  eV for our study.

## IV. STATISTICAL TESTS

We use the two-dimensional KS test [44, 45] to test whether the AGASA UHECR events above  $4 \times 10^{19}$  eV are consistent with the cosmic-ray intensity distribution predicted by the GRB and magnetar models in infrared bright spirals discussed in Secs. II and III. In this section we first describe our calculations of the expected UHECR distribution from the models and then discuss the statistical test and the results.

### A. Model Predictions

The spectrum of cosmic rays at Earth depends on both the injection spectrum at the acceleration sites and possible particle interactions that would degrade the energies of the primaries between the source and Earth. As discussed in Sec. II, we model the injection spectrum to be  $f(E_i) = E_i^{-p}$ ,  $p = 2 - 2.5$  for the GRB models and  $f(E_i) = E_i^{-1}[1 + (E_i/E_g)]^{-1}$  for the magnetar models. For the latter we will explore the three gravitational radiation cases described in Ref. [17]: no GR loss ( $E_g \rightarrow \infty$ ), moderate GR loss ( $E_g = 3 \times 10^{20}$  eV), and strong GR loss ( $E_g = 3 \times 10^{18}$  eV). To estimate the energy degradation during propagation, we use the probability  $P_p(r, E_i; E)$  that a proton created at distance  $r$  with energy  $E_i$  would arrive at Earth with an energy greater than  $E$ . It measures the proton energy degradation due to the GZK loss processes discussed in Sec. I. The same function was used in our earlier paper [46] and has been calculated using Monte Carlo simulations [47] for the parameters considered here.

We combine the injection spectrum  $f(E_i)$  and propagation loss  $P_p$ , and calculate the cosmic ray flux at Earth [in  $(\text{eV m}^2 \text{ s sr})^{-1}$ ] by

$$F(E, \Omega) = K(\Omega) \int_0^{E_{\max}} dE_i \int_0^{R_{\max}} dr [1 + z(r)]^3 \times f(E_i) \left| \frac{\partial P_p(r, E_i; E)}{\partial E} \right|. \quad (7)$$

Here  $z$  is redshift,  $E_{\max}$  is the maximum proton injection energy, and  $K$  is a normalization constant which depends on the cosmic ray injection model and the viewing direction in the sky,  $\Omega$ . The KS test (see next subsection) depends only on the relative spatial distribution of the UHECR intensity in the sky, we therefore need not specify  $K$  in the theories.

Fig. 2 compares the cosmic ray spectrum  $F(E)E^3$  for various GRB and magnetar models. For illustrative purposes, the figure is constructed assuming isotropic injection with a uniform comoving density, i.e.,  $K$  is indepen-

dent of direction on the sky and is proportional to the average source density and the event rate per unit time at the present epoch. If UHECRs come from discrete sources such as galaxies, this procedure assigns the same cosmic ray luminosity to each source, an assumption we will relax below. The curves in Fig. 2 have been normalized so that all model predictions have the same flux at  $4 \times 10^{19}$  eV. The GZK feature at  $E \gtrsim 4 \times 10^{19}$  eV becomes more pronounced for steeper injection spectra. (We note that Fig. 2 corrects a plotting error in the low energy spectrum ( $E < 10^{19}$  eV) of the strong GR case in Fig. 1 of Ref. [17].)

Fig. 3 illustrates the expected dependence of the average UHECR flux  $\int_{E_{\min}}^{E_{\max}} F(E) dE$  on the luminosity distance,  $d_L = cH_0^{-1} (1+z)[z - z^2(1+q_0)/2 + \mathcal{O}(z^3)]$ , to the host objects for various models: GRBs with a  $E^{-2.5}$  injection spectrum (long dashed), magnetars with no GR loss (solid and dotted), and magnetars with moderate GR loss (short dashed). Two lower energy limits  $E_{\min}$  are shown for comparison for the no GR loss model. For  $E_{\min} = 10^{20}$  eV (dotted), the integrated flux falls off sharply above  $d \sim 50$  Mpc due to the GZK loss processes. For  $E_{\min} = 4 \times 10^{19}$  eV (solid), the cutoff is more gradual and occurs at a larger distance ( $d \sim 200$  Mpc).

In order to compare the distribution of UHECR events with the hypothesized discrete sources, we now need to provide an estimate of each IRAS galaxy's contribution to the UHECR flux. We do this by reinterpreting Eq. (7) to be the flux expected from each galaxy in the IRAS catalog, with the galaxies chosen to lie within the maximum GZK zone indicated by Fig. 3. That is,  $K$  in Eq. (7) is a number chosen to be proportional to the  $60 \mu\text{m}$  luminosity for each galaxy with a catalogued sky position, all within the distance  $R_{\max}$ , while the integral over  $r$  in Eq. (7) is carried out for each galaxy separately, from 0 to the luminosity distance  $d_L(z)$  of each galaxy, using the catalogued redshift,  $z$ , for that galaxy. This is done for each of the three model injection spectra of the magnetar model, and for two possible GRB injection spectra shown in Fig. 2. Finally, we smooth the galaxy model's predictions of the UHECR flux as a function of sky position to the angular resolution of the AGASA experiment, using a top hat angular smoothing profile.

We include all IRAS PSCz galaxies within  $R_{\max} = 1$  Gpc, although our results are not sensitive to this upper cutoff as long as it is greater than the GZK zone of  $\sim 200$  Mpc. We estimate  $L_{\text{FIR}}$  by using the  $60 \mu\text{m}$  flux and the flux-luminosity relationship  $L = 4\pi d_L^2 f_{\text{FIR}}$ . We use matter density  $\Omega_m = 0.35$ , cosmological constant  $\Omega_\Lambda = 0.65$ , and  $H_0 = 70 \text{ km s}^{-1} \text{ Mpc}^{-1}$ . The luminosity distance,  $d_L$  differs from linear  $d = cz/H_0$  by  $\sim 15\%$  at 1000 Mpc and by  $\sim 3\%$  at 200 Mpc. Our final results depend very weakly ( $\sim 1\%$ ) on the exact cosmological parameters assumed in the calculations.

Fig. 4a shows a linearly spaced contour map of the UHECR integrated flux predicted by our infrared galaxy source model computed from IRAS galaxies for a magnetar model (no GR case). The SFRs (and hence magnetar

rates) associated with the galaxies are assumed to be linear in  $L_{\text{FIR}}$ . For comparison, all 60 AGASA UHECR events above  $4 \times 10^{19}$  eV are superposed. Fig. 4b shows the same quantity for a GRB model with a  $E^{-2}$  injection spectrum. No corrections for the limited sky coverage and non-uniform detector efficiency in declination (see Sec III) have yet been applied.

The question at hand is, do the model and observed angular distributions of UHECR event rate on the sky significantly differ? That is, can we disprove the null hypothesis, that the AGASA events are drawn from sources located in IRAS galaxies?

## B. Kolmogorov-Smirnov (KS) Test

Since the AGASA events do not obviously point towards individual galaxies, a statistical test is needed to quantify if the AGASA events are inconsistent with the theoretical UHECR distributions shown in maps such as Fig. 4.

The two-dimensional KS test is a generalization of the much studied one-dimensional KS test. The latter has been discussed extensively in the literature and analytical proofs for its validity can be found in [48]. It is based on comparing the cumulative probability distributions of the sample  $H(x)$  and the model  $G(x)$ . If  $D_{1d}$  is the maximum absolute value of  $H(x) - G(x)$  for all  $x$ , then the probability  $P$  that  $H(x)$  and  $G(x)$  are drawn from the same underlying distribution is given by

$$\lim_{n \rightarrow \infty} P(> \sqrt{n} D_{1d}) = Q(\sqrt{n} D_{1d}) \quad (8)$$

and

$$Q(\lambda) = 2 \sum_{k=1}^{\infty} (-1)^{k-1} e^{-2k^2 \lambda^2}, \quad (9)$$

which is valid if the number of data points in the sample,  $n$ , is  $\gtrsim 80$ . Monte Carlo methods must be used to tabulate the probabilities for smaller  $n$ .

Note that a small computed value of  $P$  indicates that the null hypothesis is false, that is, the data did not come from a distribution represented by the model. Generally,  $P < 0.1$  is considered reasonable proof that the null hypothesis is false. Larger values of  $P$  simply provide evidence that the data and model are consistent; the null hypothesis has not been proved false.

The generalization of the KS test to two dimensions is not obvious because there is no unique cumulative probability distribution in more than one dimension. At least two different generalizations of the test to two dimensions have been proposed [44, 45]. Both methods have been verified with Monte-Carlo simulations although no analytical proof for their validity exists. In this paper we use the probabilities tabulated in Ref. [44]. The test computes the *difference* between the fraction of data points

and the fraction of theoretical points in each of the four quadrants of the plane of the sky centered at a data point of angular coordinates  $(x_i, y_i)$ , where the quadrants are defined by  $(x > x_i, y > y_i)$ ,  $(x < x_i, y > y_i)$ ,  $(x < x_i, y < y_i)$ ,  $(x > x_i, y < y_i)$ . This procedure is repeated for all data points,  $i = 1, n$ , resulting in  $4 \times n$  numbers for the differences between the data and model. The maximum absolute difference value is defined as  $D_{2d}$ . Monte-Carlo simulations are used to obtain the corresponding probability  $P(> \sqrt{n}D_{2d})$  for a given  $D_{2d}$  and  $n$  [44]. It is also shown in Ref. [44] that the results are almost independent of the underlying distribution function. For large  $n$ , the probability has an analytic form [49]:

$$P(> \sqrt{n}D_{2d}) = Q\left(\frac{\sqrt{n}D_{2d}}{1 + \sqrt{1 - r_{cc}^2}(0.25 - 0.75/\sqrt{n})}\right) \quad (10)$$

where  $Q(\lambda)$  is given by Eq. (9) and  $r_{cc}$  is the linear correlation coefficient of the 2-dimensional data points  $(x_i, y_i)$ ,  $i = 1, n$ :

$$r_{cc} \equiv \frac{\sum_i (x_i - \bar{x})(y_i - \bar{y})}{\sqrt{\sum_i (x_i - \bar{x})^2} \sqrt{\sum_i (y_i - \bar{y})^2}}, \quad (11)$$

where  $\bar{x}$  and  $\bar{y}$  are arithmetic means, and  $-1 \leq r_{cc} \leq 1$ . The value  $r_{cc} = 1$  is for perfectly correlated  $x$  and  $y$ , which as expected, reduces Eq. (10) to the same form as the one-dimensional expression in Eq. (8). The value  $r_{cc} = 0$  is for no correlation between  $x$  and  $y$ , as is the case for the AGASA events.

In this study, we take the data points to be the angular coordinates  $(x, y) = (\text{RA}, \text{dec})$  for the 54 AGASA UHECR events above  $4 \times 10^{19}$  eV that lie within the sky coverage of the IRAS sample. The model predictions are the UHECR intensity calculated from IRAS galaxies as discussed in Sec IVA, and further weighted by the function  $dN_t/d\theta$  in Eq. (3) to account for the non-uniform exposure of the AGASA detector in declination  $\theta$ . We determine the KS parameter  $D_{2d}$  by searching through the four quadrants centered at the coordinates (RA, dec) of each AGASA event. For each quadrant, we compute the difference between the fraction of the UHECR events that lie in that quadrant, and the fraction of the UHECR intensity predicted by the models from IRAS galaxies in the same quadrant. We then assign the maximal difference from all  $4 \times 54$  quadrants to be  $D_{2d}$ . We determine the probability  $P(> \sqrt{n}D_{2d})$  from  $D_{2d}$  by interpolating Table I of Ref. [44]. We do not use the analytic expressions in Eqs. (9) and (10) that are adopted in the algorithm of [49] because they are accurate only for  $n \gtrsim 20$  and  $P \lesssim 0.20$ . (For instance, we find a probability of 32.9% using the subroutines provided in [49] vs. 50.6% from [44] for the magnetar-no GR model discussed below.)

Our results from the KS test for various magnetar and GRB injection spectra for UHECRs are summarized in Table I. The SFR of each IRAS galaxy is assumed to be proportional to its  $L_{\text{FIR}}$ . The consistency between

models and data above  $4 \times 10^{19}$  eV is generally high with KS probabilities in the range of 50.6% to 51.7% (third column in Table I); that is, the null hypothesis, that the angular coordinates of the AGASA events come from the set of angular coordinates of the IRAS galaxies within the GZK zone, is *not* disproved. If the data set is restricted to the 8 highest energy events above  $10^{20}$  eV (out of 11 total; 3 lie outside the IRAS coverage), however, the KS probabilities dive to between 0.30% and 0.45% (fifth column); that is, the models are rejected at  $> 99.5\%$  significance level.

The assumption of  $\text{SFR} \propto L_{\text{FIR}}$  is reasonable but is subject to some theoretical and observational uncertainties ([20] and [34]). We therefore test if the KS probabilities are sensitive to the linear relation of SFR to  $L_{\text{FIR}}$  by examining some extreme cases where  $\text{SFR} \propto L_{\text{FIR}}^\alpha$ , with  $\alpha = 0, 0.5, 1, 1.5$ , and 2. Table II summarizes the results for a magnetar (no GR loss) and GRB ( $E^{-2}$ ) injection spectrum. The test shows only small variations for  $\alpha = 0, 0.5$ , and 1, with the probabilities dropping sharply only for very steep power laws to 24.1% for  $\alpha = 1.5$  and 0.56% for  $\alpha = 2$  for the magnetar (no GR loss) injection spectrum. Similar results are found for the GRB injection spectrum. We conclude from this test that our results are robust to all reasonable range of  $\alpha \sim 1$ .

Starburst galaxies are generally associated with luminous far-infrared galaxies ( $L_{\text{FIR}} \gtrsim 10^{11} L_\odot$ ) [36]. To explore a connection between these galaxies and the UHECR events, we separate all IRAS galaxies within 200 Mpc into two samples with  $L_{\text{FIR}}$  above and below  $10^{11} L_\odot$ . We find the KS probability to be 44.3% and 60.1% for the above and below  $10^{11} L_\odot$  samples, respectively. Starburst galaxies are therefore not ruled out as possible UHECR sites, although the KS probability does not favor starbursts more than ordinary IRAS galaxies. Combining the two samples gives a probability of 49.6%, which is very close to 50.6% discussed above for the galaxy sample out to 1 Gpc. This is to be expected as most contribution to the UHECR flux comes from the GZK zone as indicated in Fig. 3.

We perform the KS test on a number of additional toy models *vs.* AGASA UHECR events to explore the discriminating power of the KS method on model assumptions. In all cases we make sure to weight the theoretical predictions with the same AGASA detector exposure function  $dN_t/d\theta$  for a fair comparison. In the first toy model, we assume an isotropic distribution of cosmic ray intensity and obtain a probabilities of 46.2% and 9.1% for the UHECR events above  $4 \times 10^{19}$  and  $10^{20}$  eV respectively to have been drawn from an isotropic distribution. In the second toy model, we ignore the redshift and  $L_{\text{FIR}}$  of the IRAS galaxies and simply test their sky positions *vs.* the 54 AGASA events. We find a KS probability of 54.5% for UHECR events above  $4 \times 10^{19}$  eV and 10.9% for events above  $10^{20}$  eV. In the third toy model, we take the sky positions of the 2702 GRBs in the Burst And Transient Source Experiment (BATSE) catalog (<http://www.batse.msfc.nasa.gov/batse>). Since

TABLE I: KS probabilities for UHECR events above  $4 \times 10^{19}$  eV and above  $10^{20}$  eV and the cosmic ray intensity from various models to be drawn from the same sample.

Model	$E > 4 \times 10^{19}$ eV	$E > 4 \times 10^{19}$ eV	$E > 10^{20}$ eV	$E > 10^{20}$ eV
	$D_{2d}(n = 54)$	$P(> \sqrt{n}D_{2d})$	$D_{2d}(n = 8)$	$P(> \sqrt{n}D_{2d})$
Magnetar: no GR loss	0.1482	50.6	0.626	0.31
Magnetar: moderate GR loss	0.1472	51.7	0.615	0.39
Magnetar: strong GR loss	0.1478	51.0	0.609	0.45
GRB: $E^{-2}$	0.1475	51.5	0.626	0.31
GRB: $E^{-2.5}$	0.1474	51.6	0.627	0.30

TABLE II: KS probabilities for UHECR events above  $4 \times 10^{19}$  eV and the expected cosmic ray intensity from different SFR models to be drawn from the same sample.

Model	Magnetar: no GR	Magnetar: no GR	GRB: $E^{-2}$	GRB: $E^{-2}$
	$D_{2d}(n = 54)$	$P(> \sqrt{n}D_{2d})$	$D_{2d}(n = 54)$	$P(> \sqrt{n}D_{2d})$
$\text{SFR} \propto L^0$	0.145	55.5	0.143	57.0
$\text{SFR} \propto L^{0.5}$	0.144	55.7	0.143	57.0
$\text{SFR} \propto L^{1.0}$	0.148	50.6	0.147	51.5
$\text{SFR} \propto L^{1.5}$	0.169	24.1	0.168	26.3
$\text{SFR} \propto L^{2.0}$	0.267	0.56	0.271	0.48

the sky coverage here is 100%, we use all 60 AGASA UHECR events in this test. We obtain a KS probabilities of 42.3% ( $E > 4 \times 10^{19}$  eV) and 5.2% ( $E > 10^{20}$  eV). A realistic calculation of the correlation between the BATSE GRBs and UHECR events from AGASA gives a negative result. [50] The numbers from these three toy models are consistent with the fact that IRAS galaxies, BATSE GRBs, and the AGASA events are all nearly isotropically distributed on the sky on large angular scales [37, 51, 52]. We do emphasize that taking only the sky positions of source catalogs and correlating them with AGASA coordinates (as done in these toy models and occasionally in the literature) is naive since it ignores important energy loss processes of the primaries during their propagation and possible dependence of the UHECR flux on source properties such as their intrinsic luminosity.

## V. DISCUSSION

In this paper we have found using the two-dimensional KS test that the AGASA data for the UHECR events with  $E > 4 \times 10^{19}$  eV are consistent (at  $\sim 50\%$  significance level) with the expected cosmic ray intensity distribution in the sky predicted by models in which the acceleration mechanism for the primaries resides in GRBs or magnetars in infrared bright galaxies. When only the highest UHECR events ( $E > 10^{20}$  eV) are used, however, we find the KS probabilities to be  $< 0.5\%$ , indicating the models are rejected at  $> 99.5\%$  significance level. When the energy cut on the UHECR sample is varied to  $E > 5 \times 10^{19}$  eV,  $> 6.3 \times 10^{19}$  eV, and  $> 8 \times 10^{19}$  eV,

we find the corresponding KS probabilities to be 54.2%, 6.73%, and 0.92% for the magnetar model (no GR loss), suggesting a better correlation of the UHECR events at lower energies.

To establish whether the low KS probabilities at the highest energies are due to the paucity of data points or due to the failure of the models under consideration, we draw 100 random samples of 8 events each from the data in the energy range,  $4 \times 10^{19}$  eV  $< E < 10^{20}$  eV. There are 46 events in this energy range in the region mapped by IRAS and the KS probability is 43.3% for the magnetar with no GR version of the model. For a fair comparison with the AGASA data, we consider only those samples for which the absolute value of the linear correlation coefficient  $|r_{cc}|$  defined in Eq. (11) is less than 0.1. We find that the mean KS probability of the 100 random samples is 52.8 % with a standard deviation of 24.4 %. It is therefore unlikely (at  $\sim 2\sigma$  level) that the poor agreement between the data above  $10^{20}$  eV and the models considered here is due to the small number of AGASA events above  $10^{20}$  eV. The AUGER experiment [53] with a projected  $\sim 60$  events per year above  $10^{20}$  eV [54] will help resolve whether these highest AGASA events indeed represent a  $2\sigma$  statistical fluke. Taken at face value, however, the existing UHECR data suggest that at least the cosmic ray events above  $10^{20}$  eV do not owe their origin to long burst GRBs, rapidly rotating magnetars, or any other events associated with core collapse supernovae.

Our work can be contrasted with a previous work [55] on the correlations between the UHECR events and luminous infrared galaxies, in which the authors used the two-dimensional generalization of the Smirnov-Cramer-



von Mises test. The conclusions of the two papers are in broad agreement, although our significance levels differ from theirs partially because unlike the K-S test used here, the generalization of the Smirnov-Cramer-von Mises test to two dimensions used in Ref. [55] does not yield a unique significance level and there is a large scatter. Moreover, Ref. [55] does not exclude the AGASA data points that lie in the unmapped region of the IRAS survey. To illustrate the importance of correcting for the detector exposure, we replace the window function in Eq. (3) with a tophat function that is equal to 1 for  $-10^\circ < \theta < 80^\circ$  and zero otherwise, and find the KS probability to drop to 33.7% from 50.6% (for the magnetar model with no GR loss).

We also test the robustness of our results by using the observed window function given by Eq. (6) instead of the theoretical function in Eq. (3). We find this to have only a  $\sim 10\%$  effect, changing the KS probabilities to 55.7%, 57.5%, 45.2%, 42.8%, and 43.1% for the five injection spectra (from top down) listed in Table I.

The significance of our comparison of the angular coordinates of the UHE events on the sky to the coordinates of the IRAS galaxies relies on rectilinear particle paths through intergalactic space. Could scattering in intergalactic magnetic fields affect our conclusion? An interesting constraint on the intergalactic field and the fluctuation correlation length from the GRB model is provided by the 8 doublet and 2 triplet UHECR events occurring with  $3^\circ$  of each other on the sky [37], among a total of 92 events with  $E > 4 \times 10^{19}$  eV that have been observed over the last 40 years. Since no such close pairs of GRBs have been observed, each UHECR doublet and triplet are therefore events from the single GRBs. However, these events are separated by a decade or more, yet GRBs last dynamically only for a few months. The particles from a GRB therefore must have undergone time delays  $> 10$  years during their propagation through the intergalactic medium, an effect which requires some form of scattering along the propagation path. The same considerations apply to the magnetar model, although in contrast to GRBs, photon observations of magnetar formation do not exist, so we lack explicit observational evidence against multiple magnetars occurring within 10 year time intervals at the same angular position.

In addition, GRBs within the very high energy GZK zone are extremely rare. The GRB rate (long bursts only) is  $\sim 3.5 \times 10^{-10} \text{ Mpc}^{-3} \text{ yr}^{-1}$ . Particles with energy above  $4 \times 10^{19}$  eV must have been emitted within the GZK zone,  $D < D_{\text{GZK}} = 100 E_{20}^{-2} \text{ Mpc}$  ( $3 > E_{20} > 0.4$ ), assuming straight line propagation. Here  $E_{20}$  is the energy in units of  $10^{20}$  eV. Then an average of  $\sim 700 E_{20}/10^6$  years pass between each separate GRB contribution to the flux of such extremely high energy particles observed at Earth. Therefore at the highest energies, the contributions from the very rare nearby bursts must be spread out in time, if the observed event rate is to be attributed to this source. The magnetar model, with its larger event rate, does not require temporal dispersion of each burst of particle in-

jection in order to account for the events observed above  $10^{20}$  eV. Such dispersion is required, however, in order to account for the doublets and triplets, since each magnetar injection event lasts only a few days [17]

The most likely origin for such time delays is charged particle motion in an intergalactic magnetic field of average strength,  $B_{\text{igm}}$ , and irregularities with amplitude  $\delta B \sim B_{\text{igm}}$  and correlation length  $l_c$ . One can show, by simple random walk arguments, that since a particle is deflected by the small angle  $\delta\theta \approx l_c/r_L = (ZeB_{\text{igm}}l_c/E) \ll 1$  in crossing a single region of correlated field, the particles from an impulsive event at distance  $D$  have arrival angles smeared over an angular width  $\Theta = (Dl_c/r_L^2)^{1/2} = 0.4^\circ l_{\text{Mpc}}^{1/2} ZB_{\text{igm}}/E_{20} (D/D_{\text{GZK}})^{1/2}$ . Here  $B_{\text{igm}} = B_{\text{igm}}/10^{-10} \text{ Gauss}$  and  $l_{\text{Mpc}} = l_c/1 \text{ Mpc}$ . Simple geometry shows the time delay associated with this angular scattering to be  $\Delta T_d = (D/2c)\Theta^2 = 365(D/D_{\text{GZK}})^2 (Z^2 B_{\text{igm}}^2/E_{20}^6) l_{\text{Mpc}}$  years. At the same time, the scattering cannot smear the inferred angular position of the source by an amount substantially larger than the angular resolution of the AGASA array. The requirements  $\Theta < 3^\circ$  and  $\Delta T_d > 10$  years constrain the intergalactic field and its fluctuation correlation length to lie in the range  $8E_{20}^2 (D_{\text{GZK}}/D)^{1/2} > ZB_{\text{igm}} l_{\text{Mpc}}^{1/2} > 0.04E_{20}^3 (D_{\text{GZK}}/D)$ ,  $0.4 < E_{20} < 3$ , if an impulsive event model is to be a viable candidate for the origin of UHECR. See Ref. [56] for a complete analysis of this issue, including a discussion of likely values for the intergalactic field and the effect of transport through galaxy clusters as well as the general intergalactic medium.

To estimate how much magnetic fields can effect our results, we take all 60 AGASA data points above  $4 \times 10^{19}$  eV and randomly displace them by  $3^\circ$ . After rejecting the 6 events that fall in the unmapped region of IRAS, we find a KS probability of 46.3 % for the no GR magnetar model, a result consistent with our earlier finding. A similar analysis for the AGASA events above  $10^{20}$  eV yields a KS probability of 0.58 % comparable to the earlier 0.31 % obtained without taking into account any deflection due to magnetic fields. These results suggest that our conclusions do not depend on the deflection of cosmic rays due to magnetic fields for the values discussed in the preceding paragraphs.

## VI. CONCLUSIONS

The two dimensional KS test applied to the angular positions of the 60 AGASA events with energies above  $4 \times 10^{19}$  eV and the angular positions of the far infrared galaxies in the IRAS PCSz catalog show that the sources of these particles are consistent with impulsive events associated with core collapse supernovae. The KS probability for this association is  $\sim 50\%$ , too large to reject the hypothesis. Possible physical models of accelerators associated with such supernovae are relativistic shock ac-

celeration associated with long burst GRBs and electromagnetic processes in the relativistic winds from newly born, rapidly rotating magnetars.

However, application of the same test to the 11 AGASA events with energy above  $10^{20}$  eV yields a KS probability of  $< 0.5\%$ , showing that the existing set of super GZK events are not consistent with the GRB model, the magnetar model, or any other model based on impulsive events associated with core collapse supernovae. At the  $\sim 2\sigma$  level, this inconsistency is unlikely to have occurred by chance. However,  $2\sigma$  results in high energy particle and photon astrophysics are notorious for their lack of robustness. Therefore, this highest energy result, which uses a very small number of cosmic ray events, is perhaps best regarded as a prediction that will be tested by the AUGER experiment. That experiment will yield enough events above  $10^{20}$  eV to show whether the con-

sistency between these compact object models and the UHE data using the whole set of results from  $4 \times 10^{19}$  eV and above, or the inconsistency between models and data using only the super  $10^{20}$  eV data, is the correct conclusion.

### Acknowledgments

C.-P. M. is partially supported by an Alfred P. Sloan fellowship, a Cottrell Scholars Award from the Research Corporation, and NASA grant NAG5-12173. J.A. is partially supported by NASA grants NAG 5-12031 and HST-AR-09548.01-A, and by the Miller Institute for Basic Research in Science. We thank California's taxpayers for their indulgence.

- 
- [1] K. Greisen, Phys. Rev. Lett. **16**, 748 (1966); G.T. Zat'sepin and V.A. Kuz'min, J. Exp. Theor. Phys. Lett. **4**, 78 (1966); R.J. Gould and G. Schreder, Phys. Rev. Lett. **16**, 252 (1966).
  - [2] M. Nagano and A. A. Watson, Rev. of Mod. Phys. **72**, 689, (2000); A. V. Olinto, Phys. Rep. **333**, 329 (2000); P. Bhattacharjee and G. Sigl, Phys. Rep. **327**, 109 (2000); and references therein.
  - [3] M. Takeda *et al.* Phys. Rev. Lett. **81**, 1163 (1998); updates at website <http://www-akeno.icrr.u-tokyo.ac.jp/AGASA>.
  - [4] D.J. Bird *et al.* [Fly's Eye Collaboration], Phys. Rev. Lett. **71**, 3401 (1993); Astrophys. J. **424**, 491 (1994); Astrophys. J. **441**, 144 (1995).
  - [5] M.A. Lawrence, R.J. Reid and A.A. Watson, J. Phys. G **17**, 733 (1991); M. Ave, J.A. Hinton, R.A. Vazquez, A.A. Watson and E. Zas, Phys. Rev. Lett. **85**, 2244 (2000).
  - [6] The HiRes Collaboration, astro-ph/0208243; astro-ph/0208301.
  - [7] N.N. Efimov *et al.*, in *Proceedings of the Astrophysical Aspects of the Most Energetic Cosmic Rays* (World Scientific, Singapore, 1991).
  - [8] M.S. Longair, High Energy Astrophysics, Vol. 2, (Cambridge University Press, London, 1994); D. Fargion, R.V. Konoplich and A. Salis, Z. Phys. C **74**, 571 (1997); D. Fargion and A. Salis, Phys. Uspekhi **41**(8), 823.
  - [9] D.F. Torres, E. Boldt, H. Hamilton and M. Loewenstein, Phys. Rev. D **66**, 0203001 (2002); and references therein.
  - [10] M. Milgrom and V. Usov, Astrophys. J. **449**, L37 (1995)
  - [11] M. Vietri, Astrophys. J. **453**, 883 (1995)
  - [12] E. Waxman, Phys. Rev. Lett. **75**, 386 (1995).
  - [13] P. Meszaros, Ann. Rev. Astron. Astrophys. **40**, 137 (2002).
  - [14] T. Galama *et al.*, Nature **395**, 670 (1998); J. van Paradijs *et al.*, Science **286**, 693 (1999); K. Stanek *et al.*, Astrophys. J. **591**, L17 (2003); M. Uemura *et al.*, Nature **423**, 843 (2003); P.A. Price *et al.*, Nature **423**, 844 (2003); J. Hjorth *et al.*, Nature **423**, 847 (2003).
  - [15] A.I. Macfadyen and S.E. Woosley, Astrophys. J. **524**, 262 (1999).
  - [16] J.C. Wheeler, I. Yi, P. Hoflich and L. Wang., Astrophys. J. **537**, 810 (2000).
  - [17] J. Arons, Astrophys. J. **589**, 871 (2003).
  - [18] P. Blasi, R.I. Epstein and A.V. Olinto, Astrophys. J. **533**, L123 (2000).
  - [19] B.M. Gaensler *et al.*, Astrophys. J. **559**, 963 (2001).
  - [20] R.C. Kennicutt, Ann. Rev. of Astron. and Astrophys. **36**, 189 (1998); and references therein.
  - [21] W. Saunders *et al.*, Mon. Not. of the Royal Astron. Soc. **317**, 55 (2000).
  - [22] D.A. Frail, S.R. Kulkarni, L. Nicastro, M. Feroci and G.B. Taylor, Nature **389**, 261 (1997).
  - [23] M. Vietri, D. de Marco and D. Guetta, Astrophys. J. **592**, 378 (2003).
  - [24] M. Spada, A. Panaitescu, and P. Meszaros, Astrophys. J. **537**, 824 (2000).
  - [25] M. Schmidt, Astrophys. J. **552**, 36 (2001).
  - [26] G.J. Fishman and C.A. Meegan, Ann. Rev. Astron. Astrophys. **33**, 415 (1995).
  - [27] C.F. Kennel and F.V. Coroniti, Astrophys. J. **283**, 649 (1984).
  - [28] H.J. Völk and P.B. Biermann, Astrophys. J. **333**, L65 (1988).
  - [29] Y.A. Gallant and A.B. Achterberg, Mon. Not. of the Royal Astron. Soc. **305**, L6 (1999); A.B. Achterberg, Y.A. Gallant, J.G. Kirk and A.W. Guthmann, Mon. Not. of the Royal Astron. Soc. **328**, 393 (2001).
  - [30] M. Ostrowski and J. Bednarz, Astron. and Astrophys. **394**, 1141 (2002).
  - [31] J. Arons, in *Neutron Stars in Supernova Remnants*, ASP Conf. Series **271**, P. O. Slane and B. M. Gaensler, eds. (San Francisco: ASP), 71 (2002)
  - [32] A. Spitkovsky and J. Arons, Astrophys. J., in press.
  - [33] Blanton, M.R., Dalcanton, J., Eisenstein, D., *et al.*, Astron. J. **121**, 2358 (2001).
  - [34] E. Cappellaro, R. Evans, and M. Turatto, Astron. and Astrophys., **351**, 459 (1999).
  - [35] B.T. Soifer, D.B. Sanders, G. Neugebauer, *et al.*, Astrophys. J. **303**, L41 (1986).
  - [36] F. Mannucci *et al.*, Astron. and Astrophys. **401**, 519 (2003).
  - [37] Y. Uchihori, M. Nagano, M. Takeda, M. Teshima, J.

- Lloyd-Evans and A.A. Watson, *Astropart. Phys.* **13**, 151 (2000).
- [38] N. Hayashida *et al.*, astro-ph/0008102.
  - [39] [www-akeno.icrr.u-tokyo.ac.jp/AGASA/](http://www-akeno.icrr.u-tokyo.ac.jp/AGASA/).
  - [40] P. Sommers, *Astropart. Phys.*, **14**, 271 (2001).
  - [41] L. Anchordoqui *et al.*, astro-ph/0305158.
  - [42] M. Takeda *et al.*, *Astrophys. J.* **522**, 225 (1999).
  - [43] M. Takeda *et al.*, *Astropart. Phys.* **19**, 447 (2003).
  - [44] G. Fasano and A. Franceschini, *Mon. Not. of the Royal Astron. Soc.* **225**, 155 (1987).
  - [45] J.A. Peacock, *Mon. Not. of the Royal Astron. Soc.* **202**, 615 (1983).
  - [46] S. Singh and C.-P. Ma, *Phys. Rev. D* **67**, 023506 (2003).
  - [47] Z. Fodor and S. Katz, *Phys. Rev. D* **63**, 023002 (2001).
  - [48] e.g., J.C.W. Rayner and D.J. Best, *Smooth Tests of Goodness of Fit*, (Oxford University Press, 1989).
  - [49] W.H. Press, S.A. Teukolsky, W.T. Vetterling, B.P. Flannery, *Numerical Recipes in FORTRAN 77*, (Cambridge University Press, 1992).
  - [50] N.W. Evans, F. Ferrer, and S. Sarkar, *Phys. Rev. D* **67**, 103005 (2003).
  - [51] W. Sutherland *et al.* *Mon. Not. of the Royal Astron. Soc.* **308**, 289 (1999).
  - [52] M.S. Briggs *et al.* *Astrophys. J.* **459**, 40 (1996); and references therein.
  - [53] [www.auger.org](http://www.auger.org).
  - [54] Auger Collaboration, T. Dova *et al.* in *Proc. 27th International Cosmic Ray Conference*, Hamburg, 2001.
  - [55] A. Smialkowski, M. Giller, and W. Michalak, *J. Phys.* **G28**, 1359 (2002).
  - [56] P. Blasi and D. De Marco, astro-ph/0307067.

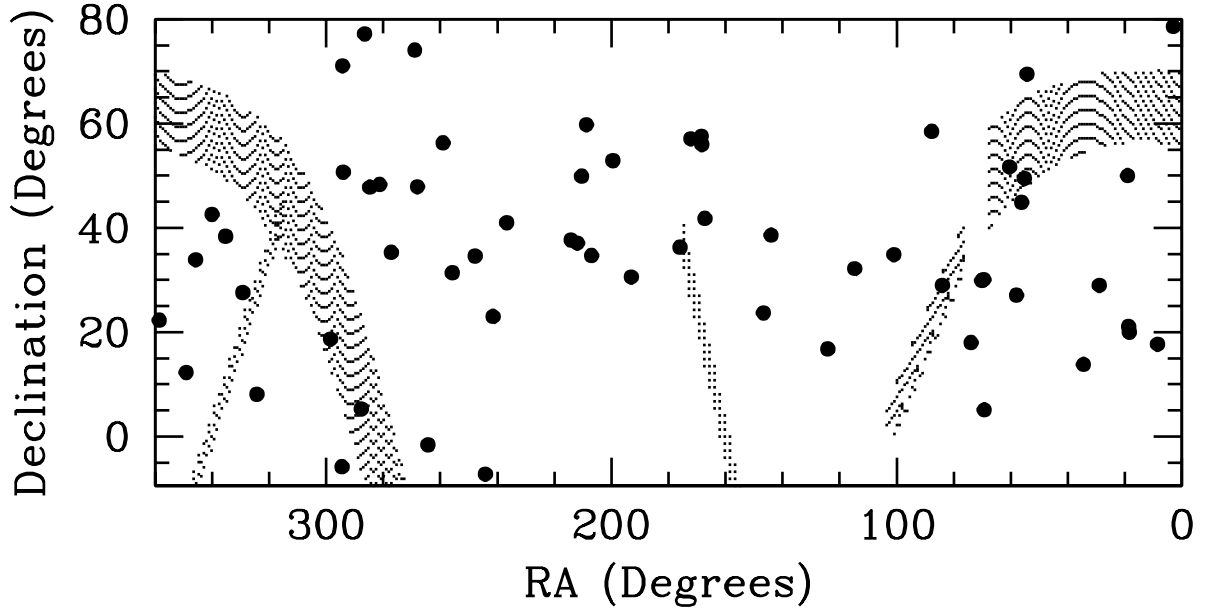


FIG. 1: Sky distribution of the 60 AGASA data points above  $4 \times 10^{19}$  eV (filled circles) and the approximate areas not mapped by IRAS (black bands). Six AGASA events lie in the unmapped IRAS region, which we exclude from our study.

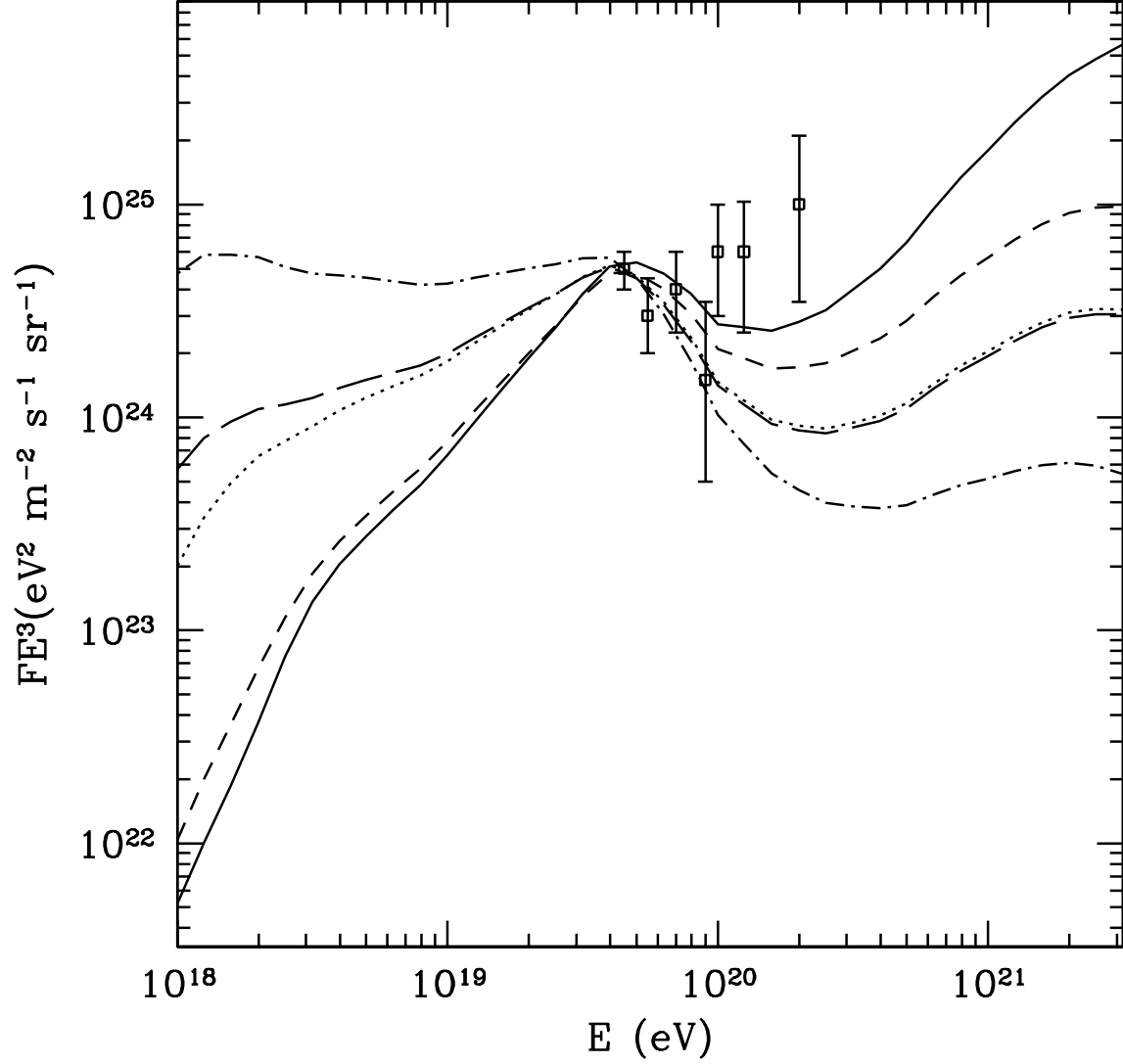


FIG. 2: Predictions for the cosmic ray flux as a function of energy assuming an isotropic distribution of sources with uniform comoving density for the five different injection spectra analyzed in this work: magnetar models with no GR loss (solid), moderate GR loss (short dashed), and strong GR loss (dotted), and GRB models with  $E^{-2}$  (long dashed), and  $E^{-2.5}$  (dot dashed). The data points (squares) are taken from Ref. [43] for an earlier set of 30 AGASA UHECR events. The GZK suppression is more important for steeper injection spectra.

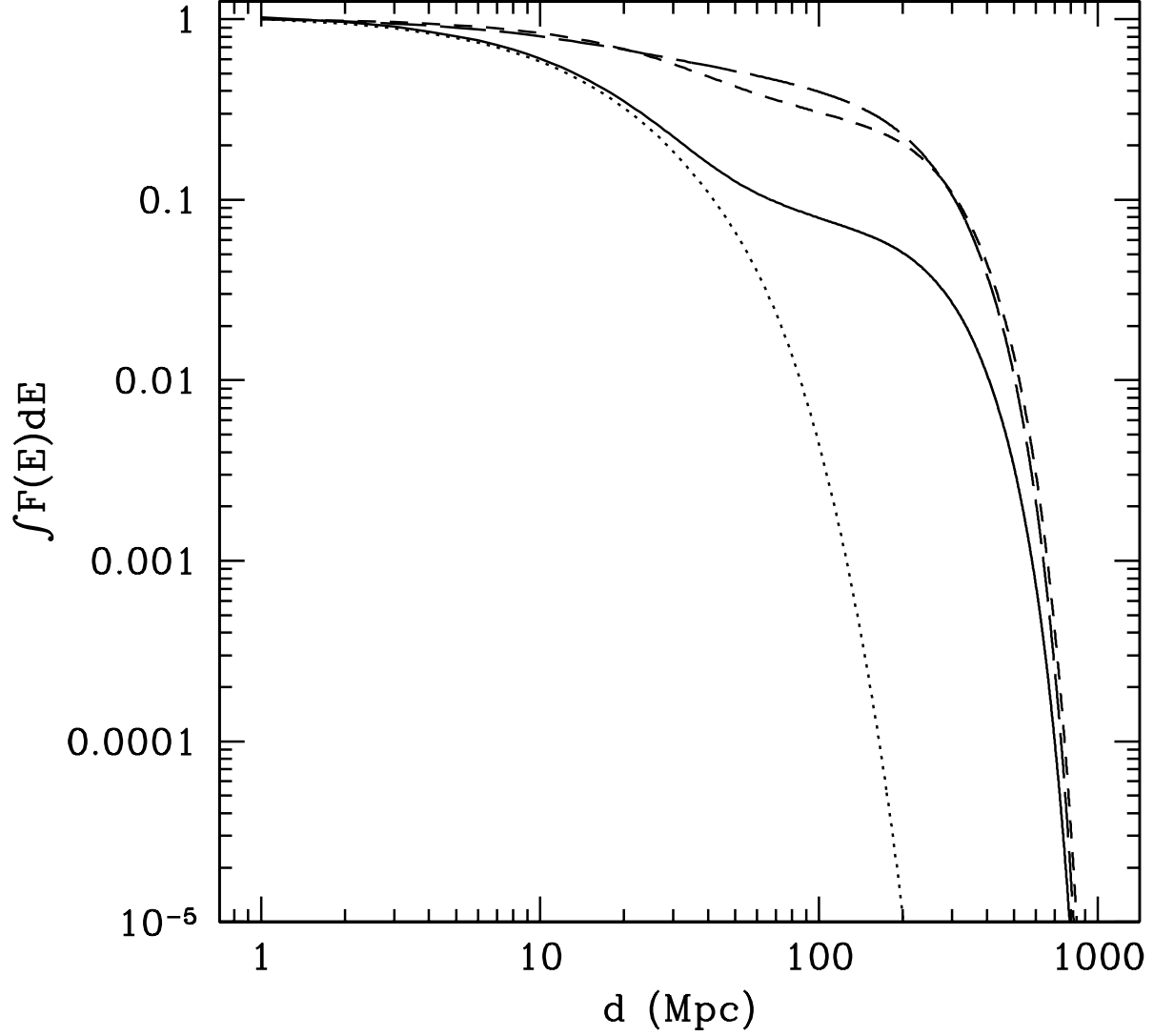


FIG. 3: The integrated flux as a function of the source distance for the no GR loss injection spectrum for  $E > 4 \times 10^{19}$  eV (solid) and  $E > 10^{20}$  eV (dotted). In the latter case the integrated flux falls off very sharply for  $d > 50$  Mpc. Also shown are the integrated flux above  $E > 4 \times 10^{19}$  eV for the moderate GR (short dashed) and  $E^{-2.5}$  (long dashed) injection spectrum. The upper cutoff in the injection spectrum was taken to be  $3 \times 10^{22}$  eV for all cases in accordance with [17].

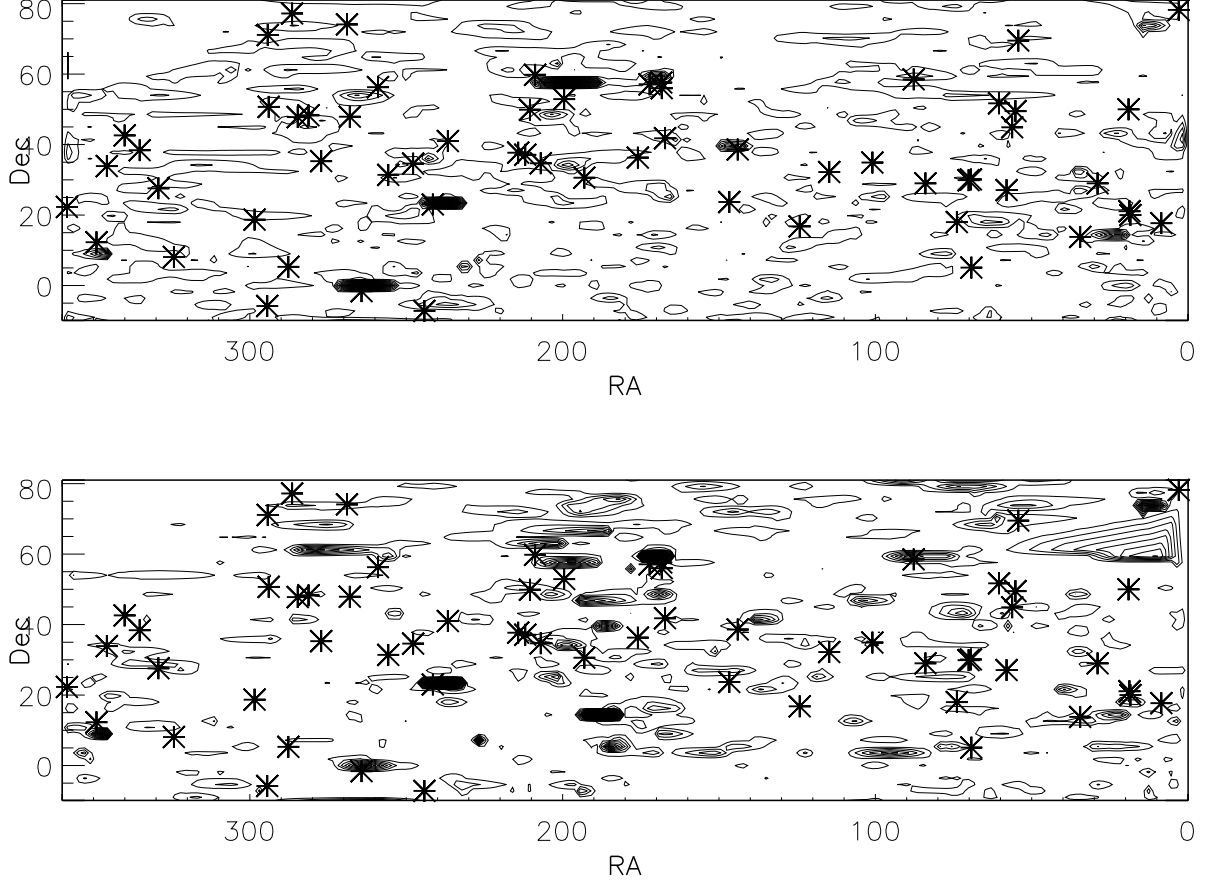


FIG. 4: Contour plot of the expected integrated cosmic ray flux from IRAS galaxies smoothed to the AGASA angular resolution of  $1.8^\circ$ . The 60 AGASA UHECR events above  $4 \times 10^{19}$  eV are shown as stars. Two models are shown for comparison: the magnetar model with no GR loss (top) and the GRB model with  $E^{-2}$  injection spectrum. No corrections for the incomplete IRAS sky coverage and non-uniform AGASA detector efficiency in declination (see Sec III) have been applied.